

# Hydrostatic and osmotic pressure activated channel in plant vacuole

Joel Alexandre and Jean-Paul Lassalles

Laboratoire "Echanges Cellulaires," URA CNRS 203, Faculté des Sciences de Rouen, BP 118, 76134 Mont-Saint-Aignan Cedex, France

**ABSTRACT** The vacuolar membrane of red beet vacuoles contains a channel which was not gated by voltage or  $\text{Ca}^{2+}$  ions. Its unit conductance was 20 pS in 200 mM symmetrical KCl solutions. It was stretch activated: the conductance remained constant but the probability of opening was increased by suction or pressure applied to a membrane patch. A  $1.5\text{-kNm}^{-2}$  suction applied to isolated patches or a  $0.08\text{-kNm}^{-2}$  pressure applied to a  $45\text{-}\mu\text{m}$  diameter vacuole induced an e-fold change in the mean current. A 75% inhibition of the channel current was obtained with  $10\text{ }\mu\text{M}$   $\text{Gd}^{3+}$  on the cytoplasmic side. The channel was more permeable for  $\text{K}^+$  than for  $\text{Cl}^-$  ( $P_{\text{K}}/P_{\text{Cl}} \sim 3$ ). A possible clustering for this channel was suggested by the recordings of the patch current. The channel properties were not significantly affected by a change in sorbitol osmolality in the solutions under isoosmotic conditions, between 0.6 and 1 mol/kg sorbitol. However, the channel was very sensitive to an osmotic gradient. A  $0.2\text{-mol/kg}$  sorbitol gradient induced a two-fold increase in unit conductance and a thirty-fold increase in the mean patch current of the channel. A current was measured, when the osmotic gradient was the only driving force applied to the vacuolar membrane. The hydrostatic and osmotic pressure (HOP) activated channel described in this paper could be gated *in vivo* condition by a change in osmolality, without the need of a change in the turgor pressure in the cell. The HOP channel represents a possible example of an osmoreceptor for plant cells.

## INTRODUCTION

There are three types of energy used to gate channels in cell membranes: the chemical energy through binding of the channel with a ligand; the electrical energy through membrane potential and the mechanical energy through membrane stretch. Ligand and voltage-dependent channels have already been detected in the vacuolar membrane of plant cells. An example of a ligand gated channel is given by the  $\text{Ca}^{2+}$  selective channel found in the tonoplast of isolated red beet vacuoles (1). This channel is opened by micromolar concentration of Inositol 1,4,5 trisphosphate, an intracellular second messenger involved in a  $\text{Ca}^{2+}$  based transduction pathway (2).

The probability of opening for several channels is strongly voltage dependent (1, 3–6), but the biological importance of gating by voltage in vacuoles is less obvious. An electrical gate would imply a shift from positive to negative values of the vacuolar potential whereas *in vivo*, its value is assumed to be positive.

Gating of channels in the tonoplast by osmotic or hydrostatic pressure can be suspected because of the importance of the vacuole in the control of water movement. A pressure-activated channel has already been found in the plasma membrane of tobacco cells (7), but to our knowledge, such a channel was never mentioned on plant vacuoles. The direct gating of channels by osmotic pressure has also been studied on theoretical

grounds (8) but nonphysiological large changes in osmolality seem to be required to open the channels (9).

In the experiments reported here, we present the effect of osmotic and hydrostatic pressure on two types of channels found in isolated red beet vacuoles.

## METHODS

### Electrophysiological recordings

Standard patch-clamp techniques (10) were applied to isolated vacuoles. Pipettes were pulled (PP83 Narishige USA, Inc., Greenvale, NY) from soft glass microhematocrit capillary (Blu-Tip, Monoject Scientific, Division of Sherwood Medical ATHY Co., Kildare, Ireland). The tip diameter of the pipettes, as estimated from bubble index measurements in methanol (11) was in the range 0.5 to  $1.5\text{ }\mu\text{m}$ , corresponding to an electrical resistance of  $10\text{ M}\Omega$  to  $1\text{ M}\Omega$  in 200 mM KCl. The 1–3  $\text{M}\Omega$  pipettes were used for the "whole-vacuole" recordings, making the voltage clamp error  $< 3\text{ mV}$  for the largest current used ( $\sim 10^{-9}\text{ A}$ ). Pipettes were not fire polished but were coated with silane; after filling a pipette, its tip was dipped for a few seconds in a 30% chlorotrimethylsilane, 70% carbon tetrachloride solution and air dried. In most cases gentle suction resulted in a giga-seal ( $> 10\text{ G}\Omega$ ) between the pipette and the vacuolar membrane. Application of voltage pulses (1V, 50 ms) to this vacuole-attached patch consistently yielded the whole-vacuole configuration. Pulling the pipette away from the vacuole in this case always resulted in an outside-out patch, at the cytoplasmic side of the tonoplast facing the pipette solution. Once pulled from a vacuole-attached patch, an outside-out patch was still obtained quite frequently (30–50%) whereas an inside-out patch is usually expected in

this case (10). The experiments were carried out at room temperature (20–22°C) with an RK300 amplifier (Biologic, Claix, France). Current measurements were stored on a Sony SLT50 video tape recorder via a modified Sony PCM-501 pulse code modulator (Biologic). These data were low-pass filtered (400 Hz for isolated patch current; 10 Hz for whole-vacuole current) with an eight-pole Butterworth filter (Kemo Ltd., UK) to an HP 98580 microcomputer. Analysis for amplitude distribution of the current in isolated patches was done with Biologic software. Electrical connections were made via Ag-AgCl wires. The bath was grounded via a reference electrode (an electrode with a broken tip filled with the bathing solution). When the bath was occasionally perfused with a second solution, the reference electrode was not modified. The reversal potentials were not corrected for the diffusion potentials; when estimated with the Planck-Henderson equation, they were <0.4 mV for the solutions used. The glass bottom of the experimental chamber was washed with ethanol before use for electrophysiological experiments. It was found that vacuoles more easily adhered on the glass bottom in this case. When a change in the bath solution was needed in the whole-vacuole experiments, the experimental chamber (150  $\mu$ l) was perfused at 100–250  $\mu$ l min<sup>-1</sup>. For isolated patches experiments, it was possible to get the pipette very close from the chamber input for solution: modifications of the channel current were frequently observed in less than a few seconds. When a high resolution in current was necessary, perfusion was stopped to reduce 50 Hz noise. Current/potential ( $I/V$ ) curves in the whole-vacuole configuration were obtained as follows. The voltage was clamped from -60 mV to +60 mV in 10 mV, 30 s steps. For each potential, the steady-state value for the current was always reached in <30 s (command voltage pulses were provided by a programmable stimulator (PS, Biologic). For isolated patches an  $i/V$  curve was obtained by measuring the single-channel current,  $i$ , for various pipette potential between -60 mV and +60 mV. Sign conventions use the cytoplasmic side as reference, so that positive pipette voltage means vacuolar side positive to cytoplasmic side. Positive currents mean currents moving from the vacuolar side to the cytoplasmic side: they correspond to upward deflections on the recordings. In the current/pressure curves, the vacuolar potential was first clamped at the selected potential (whole-vacuole configuration), and the steady-state current was measured for different values of the pipette pressure (pipette pressure defined as pressure in the pipette–pressure in the external medium) from 0 to 0.8 kNm<sup>-2</sup> (1 cm Hg = 1.33 kNm<sup>-2</sup>). The current usually reached a plateau in <20–30 s. Modifications of the pipette pressure to activate channels in the tonoplast were applied by mouth or syringe (12) and gauged with a U tube filled with Hg (isolated patches) or with water (whole-vacuole recordings). The pipette pressure used in the experiments was positive for the whole-vacuole recordings and negative for the isolated patches, corresponding to a suction.

## Preparation of vacuoles

Red beet vacuoles contain the natural pigments betacyanin and betaxanthin. The vacuoles are easily distinguished in the light microscope because of the occurrence of these natural markers. The method used to prepare isolated vacuoles is adapted from the Leigh and Branton (13) isolation procedure. A thick slice (diameter 6–8 cm; thickness 5 mm) of red beet tissue was removed perpendicular to the plant axis and midway between the two ends of the beet and was placed in a plastic dish. 5 ml of an EDTA solution (5 mM EDTA; 0.7 mol/kg sorbitol; 50 mM Tris-Mes pH 7.5) was poured to cover the slice with a layer of solution. 30 min later, the slice was cut in 20–30 pieces. After 30–40 min, most of the vacuoles released in a sample of the medium were similar in size and color to the vacuoles observed in intact cells. The diameter of the vacuoles ranged between 30 and 100  $\mu$ m and their color varied from pink to dark red. Vacuoles were

smaller and the yield was negligible when the sample was collected in an EDTA free solution or when it was collected only a few minutes after cutting the beet tissue. For our experiments, individual vacuoles were selected according to their mean diameter:  $45 \pm 5 \mu$ m. These vacuoles could differ according to their color and membrane elasticity. The membrane stiffness was not measured but some hints on its variation from vacuole to vacuole were brought about by the mechanical behavior of the vacuolar surface under a liquid stream flowing from a patch pipette. When the membrane surface was located a few microns from the tip of the pipette, the same stream induced a local modification of the vacuolar surface, from barely visible to a 5- $\mu$ m deep depression.

A micrometer eyepiece was used to measure the vacuolar diameter under microscope (Nikon Diaphot with a long working distance 40 $\times$  objective). The vacuoles were sucked into a micromanipulated (De Fonbrune) pipette and transferred to the recording chamber.

## Preparation of the solutions

Solutions were prepared as follows: (a) pH buffers: pipette medium:  $5 \times 10^{-3}$  M Mes, pH adjusted to 5.5 with Tris; external medium:  $5 \times 10^{-3}$  M Tris, pH adjusted to 7.5 with Mes; (b) Ca<sup>2+</sup> buffer: a  $10^{-7}$  M-free Ca<sup>2+</sup> external medium was obtained by replacement of the usual  $10^{-3}$  M CaCl<sub>2</sub>, with  $1.5 \times 10^{-3}$  M CaCl<sub>2</sub> and  $2 \times 10^{-3}$  M EGTA, assuming a value of  $2.6 \times 10^{-8}$  M for the apparent dissociation constant of Ca<sup>2+</sup> and EGTA at pH 7.5 (14).  $10^{-3}$  M CaCl<sub>2</sub> solutions were unbuffered; and (c) Sorbitol osmolalities: dry sorbitol was added to prepared ionic solutions to prevent changes in ionic activities (9) when sorbitol osmolalities were varied in both pipette and external solutions.

## Calculations

Lines best fit to data were obtained by an algorithm (Marquardt-Levenberg) fitting a linear or a nonlinear equation to data. Mean patch currents,  $\bar{i}$ , under steady-state conditions is usually calculated from 200-s time recordings:

$$\bar{i} = \frac{1}{200} \int_{(200)} i(t) dt.$$

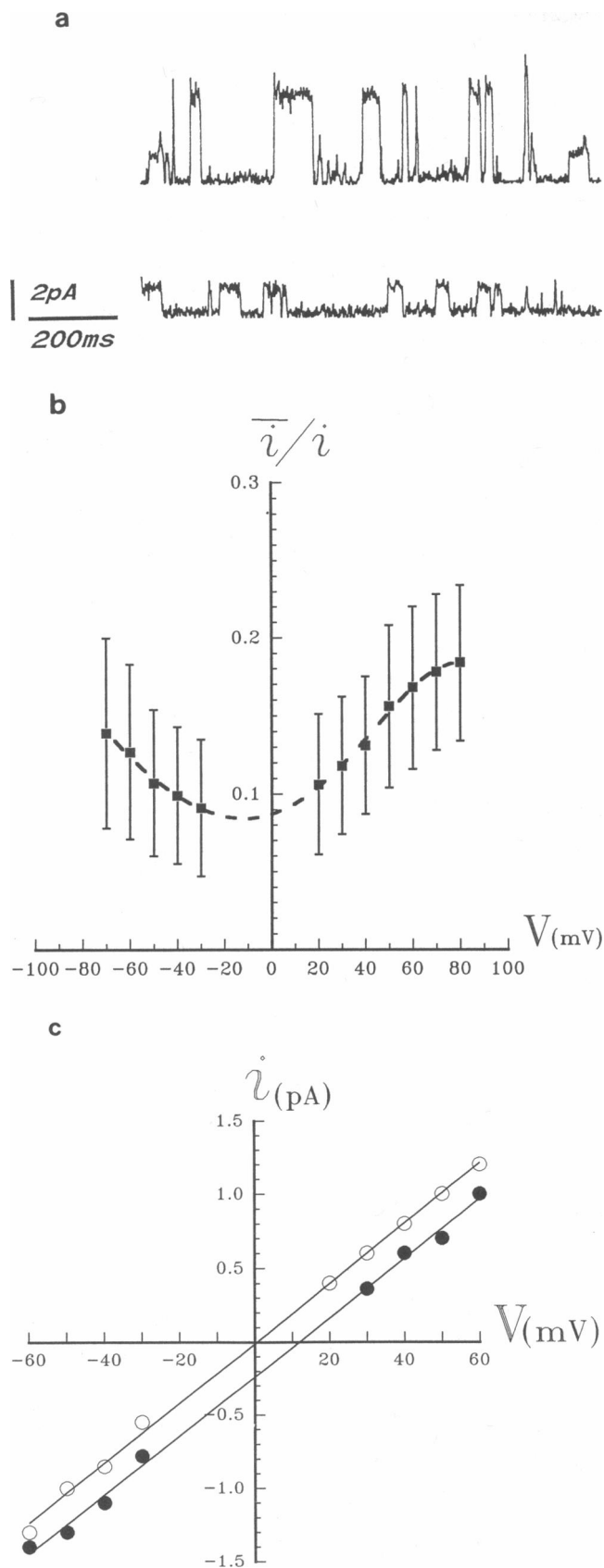
The decrease in  $\bar{i}$  induced by  $10^{-6}$  M GdCl<sub>3</sub> is defined as:

$$100 \times \frac{\text{mean value with Gd}^{3+} \text{ in the medium}}{\text{mean value without Gd}^{3+} \text{ in the medium}}$$

## RESULTS

Two types of channels were found on isolated patches of red beet vacuole without the application of osmotic or hydrostatic gradient. Fig. 1 represents the two different current levels which were sometimes visible on the same patch. For positive values of the pipette potential, an increase in external Ca<sup>2+</sup> suppressed the higher current level while the smaller one was not affected (Fig. 1 a lower curve).

From all of the isolated patches tested under the various external conditions described below, 20–30% of the patches, for which a good seal was established,



remained silent when the pipette potential was varied from  $-80$  mV to  $+80$  mV. The mean steady-state activity for active patches was slightly voltage dependent in the voltage range tested (Fig. 1 b).

In the vacuole-attached patches (data not shown), activity was always larger at  $-80$  mV than at  $+80$  mV, so we used this criterion to make the difference between inside and outside-out patches (see Methods). The channel conductance was calculated from vacuole-attached and isolated-patch measurements. For the two-patch configurations, conductance was 20 pS with 200 mM KCl in the pipette and in the external medium (Fig. 1 c). The same experiments performed in 100 mM KCl symmetrical solutions gave a 10 pS conductance value (data not shown).

### Effect of hydrostatic pressure on currents

Application of suction to isolated patches resulted in the opening of ion channels in 30–40% of attached or isolated patches. Before application of suction, the patch current was recorded for 4 min, voltage being clamped to  $+30$  mV. If the patch remained silent during that time, it was not possible to open channels by suction or pressure. When channel openings were already present in the patch, suction strongly increased the patch current in a reversed manner (Fig. 2 a). With constant pressure and voltage applied to the patch, there was no inactivation of the mean patch current for 100 s time recordings.

The effect of an excess pipette pressure was tested on a few isolated or attached patches. A similar increase in the current was obtained with a suction or with the corresponding excess pressure applied to the patch (data not shown). However, no systematic study of the patch current was performed with the excess pipette pressure.

**FIGURE 1** Isolated patch currents in red beet vacuoles. (a) A typical recording of an isolated patch shows two current levels in  $10^{-7}$  M free  $Ca^{2+}$  external medium (*upper recording*). Only the smaller level is left in  $10^{-3}$  M  $Ca^{2+}$  external medium (*lower recording*). The pipette potential is  $+50$  mV for each recording. (b) quantitation of  $\bar{i}$ , average steady-state value for the current in isolated patches with  $10^{-3}$  M  $Ca^{2+}$  in the external medium. Four recordings of patches showing only one current level for each potential in the range  $-70$  mV,  $+80$  mV were used to calculate  $\bar{i}$  in each case ( $i$ ; single-channel current). The recording time was 200 s for each value of the selected pipette potential  $V$ . ■: mean value of the ratio  $\bar{i}/i$ ; bars represent  $\pm$  s.d. (c) Open channel  $i/V$  relation for an isolated patch (○) and a vacuole-attached patch (●) with  $10^{-3}$  M  $Ca^{2+}$  in the external medium.

For all experiments: external medium: 0.6 mol/kg sorbitol, 0.2 M KCl,  $2 \times 10^{-3}$  M  $MgCl_2$ , pH 7.5. Pipette medium: 0.6 mol/kg sorbitol, 0.2 M KCl,  $2 \times 10^{-3}$  M  $MgCl_2$ ,  $10^{-3}$  M  $CaCl_2$ , pH 5.5 (○) or pH 7.5 (●).

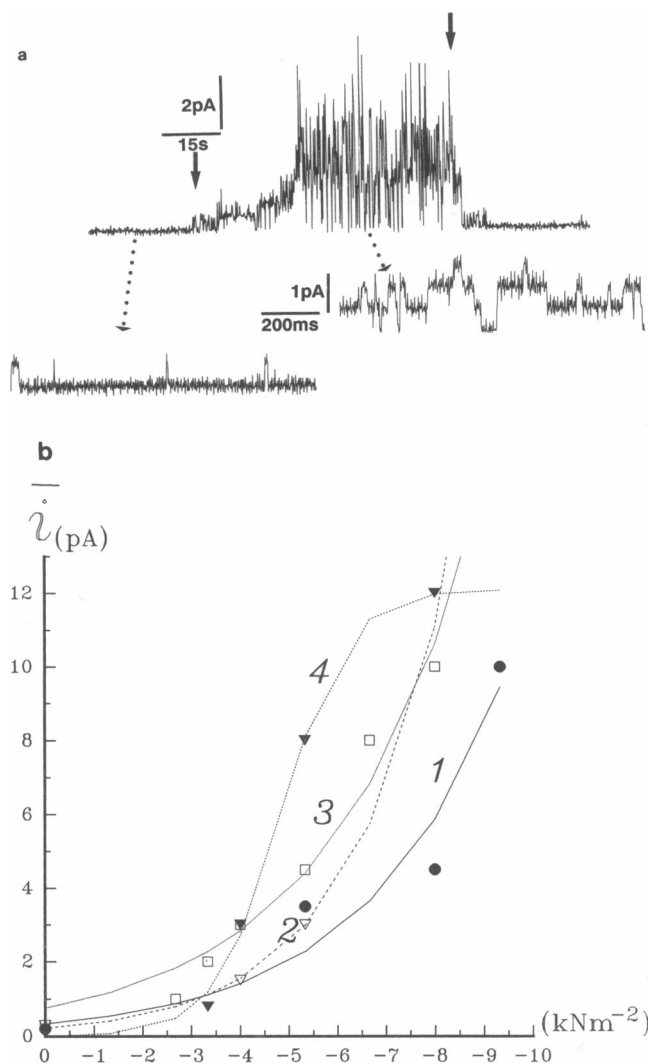


**FIGURE 2** The effect of suction on isolated patch recordings. (a) Response to suction in a patch. Suction was slowly increased from 0 to  $5.33 \text{ kNm}^{-2}$  at the first arrow and sharply released at the second arrow (upper curve). Lower left and right curves represent enlarged sections of the upper curve before and after application of suction. (b) Dependency of the mean patch current  $\bar{i}$ , with suction. Symbols  $\blacktriangledown$ ,  $\square$ ,  $\blacktriangledown$  and  $\bullet$  represent four different patches. Curves 1, 2, 3 are the best fit to equation:  $\bar{i} = Ae^{\theta P}$ ; curve 4 is the best fit to equation:  $\bar{i} = B/(1 + Ce^{-\theta P})$ .  $P$ : suction ( $\text{kNm}^{-2}$ ),  $\bar{i}$ : mean patch current, calculated from a 200 s recording of the patch current at the selected suction  $P$  applied to the patch.  $A$ ,  $B$ ,  $C$ ,  $\theta$ : parameters of the fit. The nonlinear algorithm used for curve fitting gives the best value of  $\theta$  ( $\text{kN}^{-1}\text{m}^2$ ) for each patch: curve 1:  $\theta = 0.35$ , curve 2:  $\theta = 0.49$ , curve 3:  $\theta = 0.33$ , curve 4:  $\theta = 1.46$ .

For all experiments, pipette potential:  $V = +30 \text{ mV}$ ; External medium:  $0.6 \text{ mol/kg}$  sorbitol,  $0.2 \text{ M KCl}$ ,  $2 \times 10^{-3} \text{ M MgCl}_2$ ,  $10^{-3} \text{ M CaCl}_2$ , pH 7.5. Pipette medium:  $0.6 \text{ mol/kg}$  sorbitol,  $0.2 \text{ M KCl}$ ,  $2 \times 10^{-3} \text{ M MgCl}_2$ ,  $10^{-3} \text{ M CaCl}_2$ , pH 5.5.

Because pressure changes in the pipette were applied by mouth or syringe, it was not possible to measure pressure during the transient; only mean steady-state values of the current, corresponding to established values of suction in the pipette, were used (Fig. 2 b). Maximum suction sustained by a patch before breaking the seal or the patch membrane was  $8\text{--}10 \text{ kNm}^{-2}$ . Usually the highest values for suction were not sufficient to induce saturation in current (except perhaps for patch  $n^{\circ}4$  Fig. 2 b). Suction had no effect on the conductance of the channel. This can be seen (a) on the lower recordings Fig. 2 a: the open levels induced by suction are evenly spaced and correspond to the open level before suction (b) on the measurements of conductance given in Fig. 4 b: no important change in the  $i/V$  curve is found before and after application of a  $6 \text{ kNm}^{-2}$  suction on an isolated patch. When the  $\text{Ca}^{2+}$  sensitive channel was also present in a patch under the ionic conditions of Fig. 1, it was found that this channel was not sensitive to suction or excess pressure.

A patch usually contains many channels which are activated by suction in a strong nonlinear manner (Fig. 2 b). This is the case even if there is only one open current level on the recording when there is no applied suction to the patch (Fig. 2 a). The fits to data are discussed in the next part of this paper.

Application of excess pressure to the pipette was used to modify the vacuolar current (Fig. 3) at  $+50 \text{ mV}$ . For the five vacuoles tested, there was a wide variation in the response. When vacuoles were submitted to the same  $0.5 \text{ kNm}^{-2}$  pressure, the current values ranged between  $200\text{--}1,200 \text{ pA}$ . As for the isolated patches, it was not always possible to reach the saturation value for the current because of the breaking of the seal or of the vacuolar membrane (the break clearly occurred in the vacuolar membrane, far from the seal itself, in only one of the experiments).

To record the pressure sensitive current between  $-60$  and  $+60 \text{ mV}$ ,  $\text{ZnCl}_2$  was used to prevent opening of  $\text{Ca}^{2+}$  sensitive channels for negative voltages (15). Under the ionic conditions of Fig. 3 b (symbols  $\bullet$ ), in the lack of applied pressure, the vacuolar current was always  $< 50 \text{ pA}$ . The pressure induced current was sensitive to the pipette potential especially for the positive values of this potential (symbols  $\blacktriangledown$ ,  $\nabla$ ).

Reversal potentials were measured on a vacuole clamped at zero current value with a pressure of  $0.6 \text{ kNm}^{-2}$  applied to the pipette. With  $20 \text{ mM KCl}$  in the pipette and  $100 \text{ mM}$  or  $200 \text{ mM KCl}$  in the external solution, the reversal potentials were respectively  $+18 \text{ mV}$  and  $+24 \text{ mV}$  corresponding to  $P_K/P_{Cl}$  ratio of 3.2 and 3.4, assuming that  $\text{K}^+$  and  $\text{Cl}^-$  are the only permeable ions in the Goldman equation.

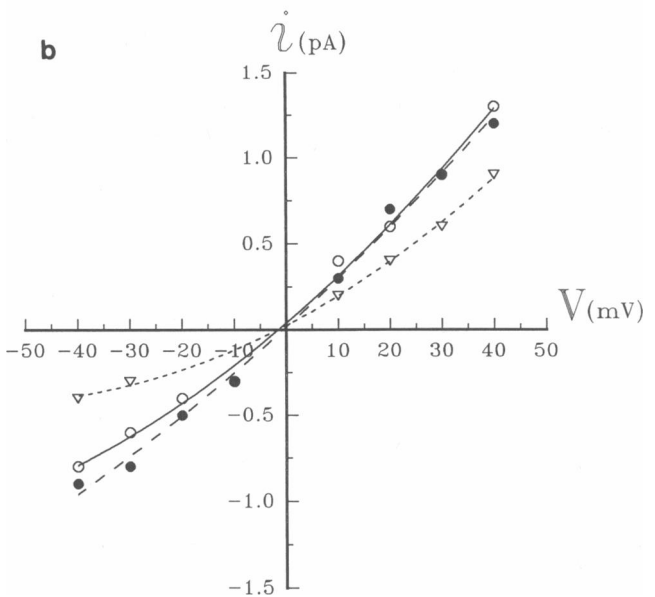
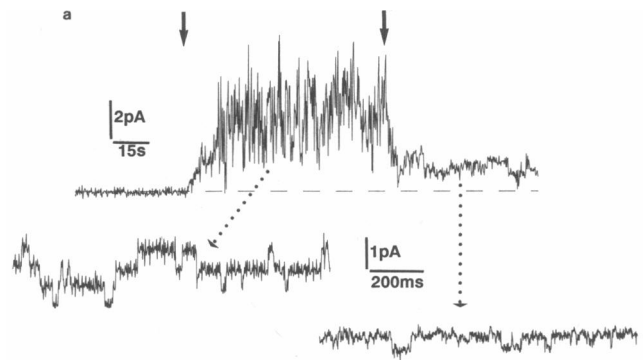
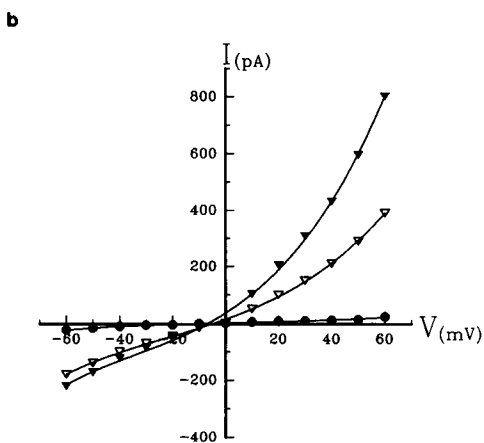
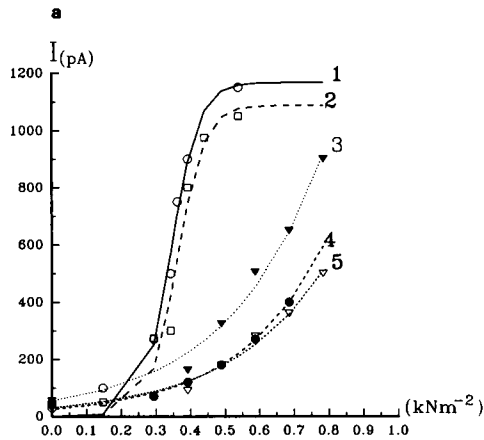


**FIGURE 3** Variation of vacuolar current with pipette pressure. (a) The vacuolar current was recorded on five vacuoles clamped at +50 mV (symbols  $\circ$ ,  $\square$ ,  $\nabla$ ,  $\blacktriangledown$ ,  $\bullet$ ) for different values of the pipette pressure. The equations given in legend Fig. 2 b were used to represent the best fit for each vacuolar current  $I$ .  $P$ : pipette pressure ( $\text{kNm}^{-2}$ ). Values for  $\theta$  ( $\text{kN}^{-1}\text{m}^2$ ): curve 1:  $\theta = 25.1$ , curve 2:  $\theta = 25.2$ , curve 3:  $\theta = 4$ , curve 4:  $\theta = 3.6$ , curve 5:  $\theta = 3.6$  (b)  $I/V$  curves for different values of the pipette pressure applied to the same vacuole. Potential was stepped from  $-60$  mV to  $+60$  mV for different pipette pressure:  $\blacktriangledown$ :  $0.4 \text{ kNm}^{-2}$ ;  $\nabla$ :  $0.2 \text{ kNm}^{-2}$ ;  $\bullet$ :  $0 \text{ kNm}^{-2}$ .

For all the experiments: external medium:  $0.6 \text{ mol/kg}$  sorbitol,  $0.2 \text{ M KCl}$ ,  $2 \times 10^{-3} \text{ M MgCl}_2$ ,  $10^{-3} \text{ M CaCl}_2$ , pH 7.5. Pipette medium:  $0.6 \text{ mol/kg}$  sorbitol,  $0.2 \text{ M KCl}$ ,  $2 \times 10^{-3} \text{ M MgCl}_2$ ,  $10^{-3} \text{ M CaCl}_2$ , pH 5.5. In (b)  $10^{-4} \text{ M ZnCl}_2$  was added in the external medium.

The effect of  $\text{GdCl}_3$  was tested on both isolated patches and whole-vacuole currents induced by pressure.  $\text{GdCl}_3$  was effective on the cytoplasmic side only and the effect was 100% reversible by washing. The patch recording in Fig. 4 a indicates that, with  $10 \mu\text{M}$   $\text{GdCl}_3$  in the external medium, the mean patch current was reduced to 30% of its initial value. For three outside-out patches tested under similar conditions ( $10 \mu\text{M}$   $\text{GdCl}_3$  in the external medium: suction  $6 \text{ kNm}^{-2}$  and

**FIGURE 4** Dependency of isolated patch current with suction and  $\text{Gd}^{3+}\text{Cl}_3$ . (a) (Upper recording) the first arrow indicates a  $5.3\text{-kNm}^{-2}$  suction applied to the patch. At the time indicated by the second arrow, the patch was washed with a  $10\text{-}\mu\text{M}$   $\text{Gd}^{3+}\text{Cl}_3$  solution, suction being maintained through the patch. Pipette potential:  $+30$  mV. The dotted line corresponds to the current level before application of suction to the pipette. (Lower recordings) enlarged sections of the upper recording with (right) or without (left)  $\text{Gd}^{3+}$  present in the external medium. (b) Open channel  $i/V$  relationship in an isolated patch. Single-channel current,  $i$ , was first recorded for various pipette potentials without applied pressure in the pipette or  $\text{Gd}^{3+}\text{Cl}_3$  in the external medium ( $\bullet$ ). A  $6\text{-kNm}^{-2}$  suction was then applied to the pipette and a new set of values for  $i$  was measured for the same set of pipette potentials ( $\circ$ ). The patch was then washed with a  $10\text{-}\mu\text{M}$   $\text{Gd}^{3+}\text{Cl}_3$  solution, the suction being maintained ( $\nabla$ ).

For all the experiments: external medium:  $0.6 \text{ mol/kg}$  sorbitol,  $0.2 \text{ M KCl}$ ,  $2 \times 10^{-3} \text{ M MgCl}_2$ ,  $10^{-3} \text{ M CaCl}_2$ , pH 7.5,  $\text{Gd}^{3+}\text{Cl}_3$ , as indicated in each case. Pipette medium:  $0.6 \text{ mol/kg}$  sorbitol,  $0.2 \text{ M KCl}$ ,  $2 \times 10^{-3} \text{ M MgCl}_2$ ,  $10^{-3} \text{ M CaCl}_2$ , pH 5.5.

pipette potential 40 mV), the mean current decreased to  $25 \pm 5\%$  of its initial value.

In the whole-vacuole recordings, residual currents were larger, with two vacuoles clamped at +40 mV (pipette pressure was  $5.33 \text{ kNm}^{-2}$  and  $10 \mu\text{M GdCl}_3$  in the external medium) the recorded currents corresponded respectively to 60% and 70% of their initial values.

A possible effect of temperature on pressure-activated channel was tested by heating vacuoles for 5 min at selected temperatures (30°C, 40°C, and 50°C) in the medium used to collect them. Vacuoles were then resuspended in experimental medium at room temperature and vacuole-attached patches were submitted to a pressure of  $5 \text{ kNm}^{-2}$ . There was no significant change in the recordings (conductance or mean steady-state current) when compared to the usual recordings obtained without preliminary heating of the vacuoles. However, the number of vacuoles surviving the heat shock decreased with temperature and no vacuole was left after heating for 5 min at 65°C.

#### EFFECT OF SORBITOL OSMOLALITY ON CURRENT

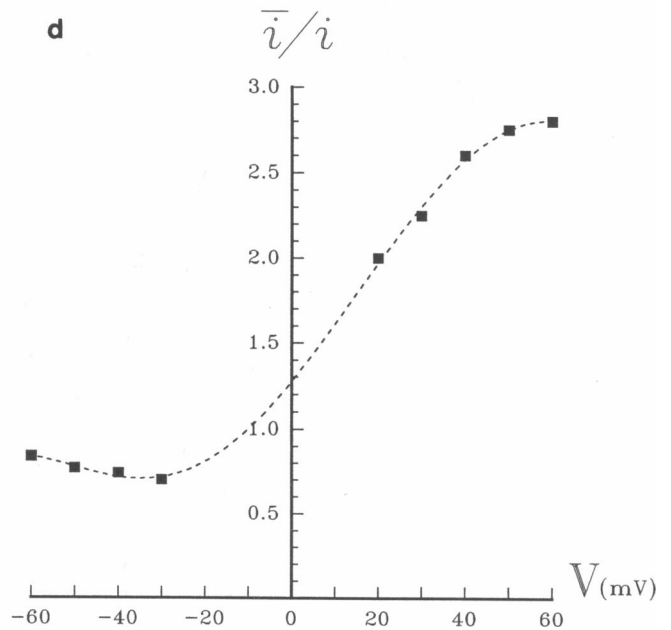
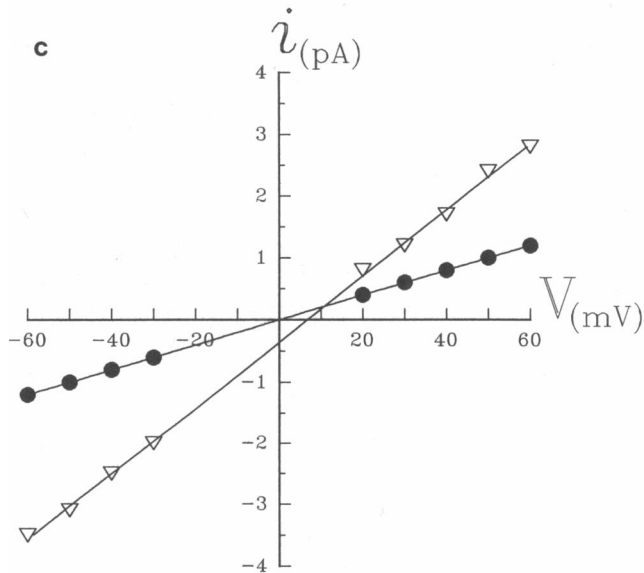
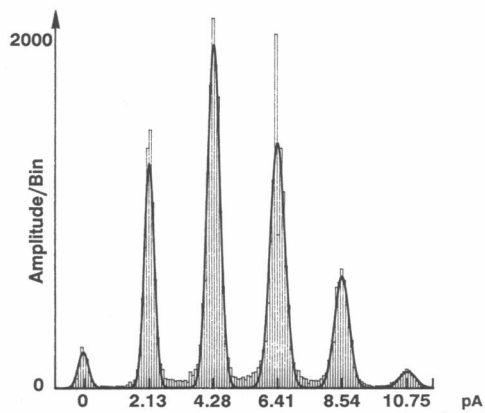
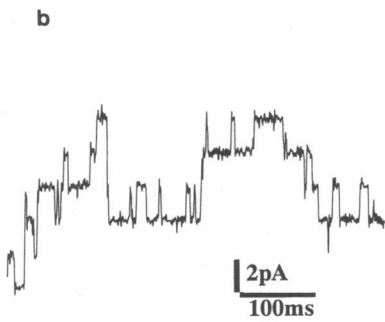
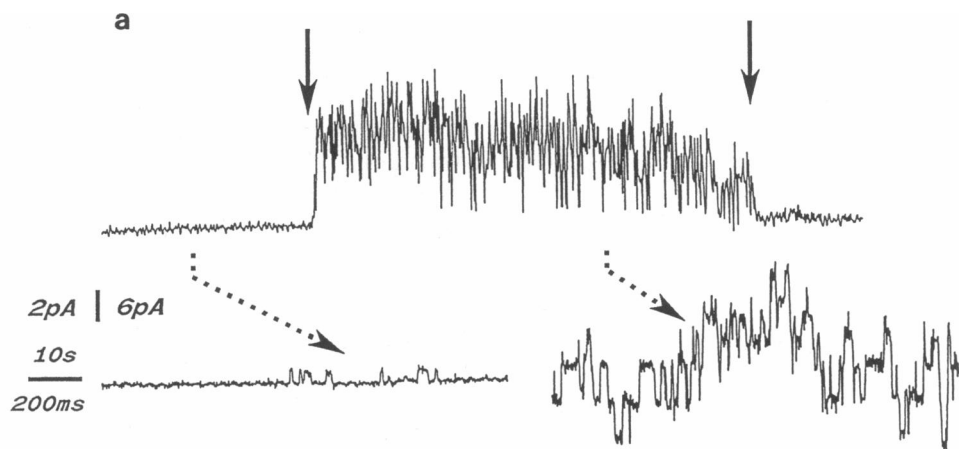
Ten patches were submitted to a 0.2 mol/kg sorbitol gradient. Three of the patches were initially performed with 0.6 mol/kg sorbitol in the pipette, in a 0.6 mol/kg sorbitol solution. The gradient was established by washing the patches with a 0.8 mol/kg sorbitol solution. An example of a current recording from these patches is given in Fig. 5a. The gradient induced a strong, reversible increase in the patch current (*first and second arrows*, Fig. 5a). Resolution of the current states was better when no perfusion was applied to the patch submitted to the sorbitol gradient (Fig. 5b). Recordings under these conditions were used to measure the channel conductances and the mean patch current (Fig. 5, b–d).

The  $i/V$  curve (Fig. 5c) obtained under isoosmotic conditions corresponds to the 20-pS channel already described in Fig. 1. Once the sorbitol osmolality in the external medium has been increased to 0.8 mol/kg, the recordings exhibit multiple conductance states of a 40 pS level (Fig. 5, a–c). The 20-pS channel cannot be detected when there is an osmotic gradient (Fig. 5b); it would correspond to a peak located at 1 pA in the histogram given Fig. 5b. The average steady-state activity of the 40-pS channel is voltage dependent (Fig. 5d), but cannot be suppressed in the voltage range tested. When there was no channel present under isoosmotic conditions, the patch remained silent when the sorbitol

osmolality in the external medium was increased to 0.8 mol/kg.

It was possible to test the effect of sorbitol osmolality on the  $\text{Ca}^{2+}$  sensitive channel described in Fig. 1. The two types of channels were present at the same time on five patches. From these recordings (data not shown), it was found that the conductance and the probability of opening for the  $\text{Ca}^{2+}$  sensitive channel were not modified by a change from 0.6 mol/kg to 0.8 mol/kg sorbitol in the external medium. Isolated patch recordings with identical sorbitol osmolalities in the pipette and in the external medium (respectively 0.6, 0.7, 0.8, 0.9, and 1 mol/kg) were used to measure the conductance of the two types of channels under the usual 200 mM KCl media. For each sorbitol osmolality tested, two experiments were performed (data not shown). With the different sorbitol osmolalities used, there was no significant modification in conductance:  $21 \pm 2.6 \text{ pS}$  ( $n = 10$ );  $71 \pm 5 \text{ pS}$  ( $n = 10$ ), for both types of channels. The opening probabilities of the two types of channels were also independent on a change in sorbitol osmolality. The patches under osmotic stress (pipette: 0.6 mol/kg sorbitol; external medium: 0.8 mol/kg sorbitol; see legend Fig. 5a for a full description of the media), were sensitive to  $\text{GdCl}_3$ . The mean current  $\bar{i}$  was reduced to  $60 \pm 5\%$  of its initial value when the patch was washed with a 0.8 mol/kg sorbitol and  $10 \mu\text{M GdCl}_3$  medium.

Both hyperosmotic and hypoosmotic stress induced an increase in the vacuolar current. This increase was larger with the hyperosmotic medium, especially for positive values of the vacuolar potential (Fig. 6a). The vacuoles submitted to an osmotic gradient were also sensitive to  $\text{GdCl}_3$ . In a vacuole clamped at +50 mV, with 0.5 mol/kg sorbitol in the pipette, and 0.7 mol/kg sorbitol in the external medium, the value for the current was decreased to 60% of its initial value after washing of the vacuole by a 0.7 mol/kg sorbitol and  $10 \mu\text{M GdCl}_3$  medium (for a full description of the media, see legend Fig. 6). When no stretch or electric field was applied to the membrane, it was still possible to record a current sensitive to sorbitol osmolality changes (Fig. 6b). There was a near linear relationship between the current and the osmolality difference in the two media. Apparently there was not such a relationship between the current and the absolute value of the vacuolar or extravacuolar sorbitol osmolality. Control experiments were performed on different vacuoles under the conditions of Fig. 3b (●) with various isoosmotic sorbitol media: 0.6, 0.7, 0.8, 0.9, and 1 mol/kg. For all these experiments, the vacuolar current was negligible when the vacuolar potential was clamped between  $-60 \text{ mV}$  and  $+60 \text{ mV}$ .



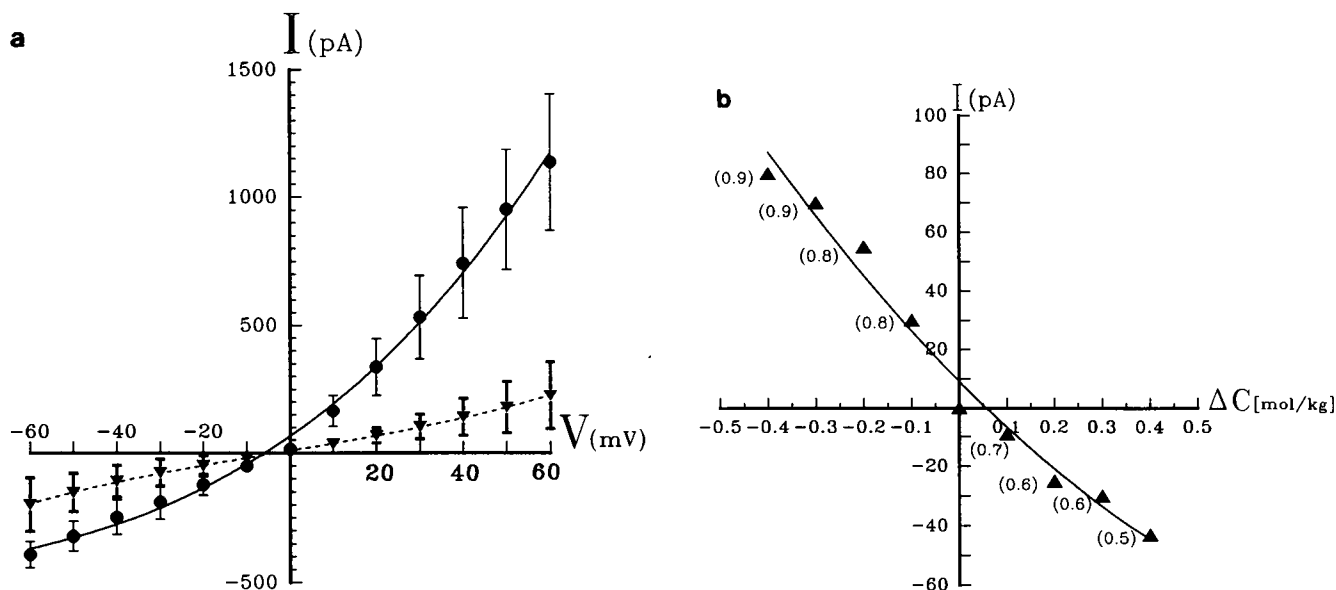


**FIGURE 6** Whole vacuole recordings with different sorbitol osmolalities in the pipette and external media. (a) Effect of sorbitol gradients on the vacuolar current for various pipette potentials. (●): 0.5 mol/kg sorbitol in the pipette; 0.7 mol/kg in the external medium. (▼): 0.9 mol/kg sorbitol in the pipette; 0.5 mol/kg in the external medium. Symbols (●, ▼) represent mean values of the vacuolar current (five vacuoles); bars correspond to  $\pm$ s.d. (b) Effect of sorbitol gradients on the vacuolar current, at zero pipette potential. For each gradient, a different vacuole was clamped at 0 mV and the steady-state value for the current was measured (symbols: ▲). Numbers into brackets represent the sorbitol osmolality in the external medium.  $\Delta C$ : sorbitol gradient expressed as: sorbitol osmolality in the pipette—sorbitol osmolality in the external medium. For  $\Delta C = 0$ , measurements were performed on the following isoosmotic media: 0.6; 0.7; 0.8; 0.9, and 1 mol/kg.

For all experiments: external medium: 0.2 M KCl,  $2 \times 10^{-3}$  M MgCl<sub>2</sub>,  $10^{-3}$  M CaCl<sub>2</sub>, pH 7.5, sorbitol osmolality: as indicated in each case. In (a)  $10^{-4}$  M ZnCl<sub>2</sub> was added to the external medium. Pipette medium: 0.2 M KCl,  $2 \times 10^{-3}$  M MgCl<sub>2</sub>,  $10^{-3}$  M CaCl<sub>2</sub>, pH 5.5, sorbitol osmolality: as indicated in each case.

## DISCUSSION

Two types of channels present in the tonoplast of red beet vacuoles are mentioned in this report. In 200 mM KCl solutions, for the positive values of the vacuolar potential, a 70 pS channel was found for the low value ( $10^{-7}$  M) of cytoplasmic Ca<sup>2+</sup>. It disappeared in  $10^{-3}$  M Ca<sup>2+</sup> solution. A 20-pS channel, was not modified by the same Ca<sup>2+</sup> change from  $10^{-7}$  M to  $10^{-3}$  M (Fig. 1 a).

In previous work on Ca<sup>2+</sup> dependent channels in sugar

beet vacuoles (3), Hedrich and Neher give evidences for two types of Ca<sup>2+</sup> sensitive channels being present in the tonoplast. When cytoplasmic Ca<sup>2+</sup> is low ( $\sim 10^{-7}$  M), a “fast vacuolar” (FV) type is activated at both negative and positive values of the vacuolar potential. When cytoplasmic Ca<sup>2+</sup> is high, a “slow vacuolar” (SV) type is activated at negative voltages. The 70-pS channel found in the red beet vacuoles could then correspond to the FV channel mentioned on the sugar beet vacuoles. However, the simpler explanation for the data that we

**FIGURE 5** Effect of sorbitol osmolalities on isolated patches. (a) Isolated patch recording during perfusion of the experimental chamber. The patch current was first recorded in a 0.6 mol/kg sorbitol solution. At the times indicated by the arrows, it was washed first with a 0.8 mol/kg, then with a 0.6 mol/kg, sorbitol solutions. Lower left and right recordings represent enlarged sections of the upper recording in 0.6 mol/kg or 0.8 mol/kg sorbitol (dotted arrows). Pipette potential: +50 mV. The horizontal calibration bar is 10 s (upper recording) or 200 ms (lower recordings). The vertical calibration bar is 6 pA (upper recording) or 2 pA (lower recordings). (b) (Right) Amplitude histogram of the different current states of an isolated patch recording without perfusion. The external medium contains 0.8 mol/kg sorbitol and the pipette potential is 50 mV. The amplitude histogram was fitted by five superimposed Gaussian functions, used to derive the following values: for the closed state,  $i_0 = 0$ ; for the open states,  $i_1 = 2.13$  pA,  $i_2 = 4.28$  pA,  $i_3 = 6.41$  pA,  $i_4 = 8.54$  pA,  $i_5 = 10.75$  pA. Total number of amplitude values: 50,000. Sampling frequency of the current recording: 1,200 Hz. Bin width: 0.252 pA. (Left) Sample of the recording used to calculate the amplitude histogram. (c)  $i/V$  relationship obtained from an isolated patch, first in a 0.6 mol/kg (●), then in a 0.8 mol/kg sorbitol (▽) medium. (d) Effect of the pipette potential on the average steady-state activity ( $\bar{i}/i$ ) of the channels in an isolated patch. External medium contains 0.8 mol/kg sorbitol.  $\bar{i}$ : mean-patch current calculated from 200 s recordings for  $V$  value of the potential. ( $i$ : value of the single-channel current for this potential).

For all the experiments: external medium: 0.2 M KCl,  $2 \times 10^{-3}$  M MgCl<sub>2</sub>,  $10^{-3}$  M CaCl<sub>2</sub>, pH 7.5, sorbitol osmolality: as indicated in each case. Pipette medium: 0.6 mol/kg sorbitol, 0.2 M KCl,  $2 \times 10^{-3}$  M MgCl<sub>2</sub>,  $10^{-3}$  M CaCl<sub>2</sub>, pH 5.5.



present in this paper is that a 70-pS channel is closed by an increase in cytosolic  $\text{Ca}^{2+}$ .

The 20-pS,  $\text{Ca}^{2+}$  insensitive channel, found in the red beet vacuoles, gives small values for the current when there is no externally applied pressure or osmotic gradients. If we assume a  $10\text{-}\mu\text{m}^2$  patch area (16), the value of the mean patch current for the 20-pS channel at +60 mV (Fig. 1, *b* and *c*) is 100 pA for a vacuole with a  $45\text{-}\mu\text{m}$  diameter. The direct measurements of this vacuolar current at +60 mV give similar values, between 30 pA and 80 pA in  $10^{-3}$  M  $\text{Ca}^{2+}$  (Fig. 3 *b*, ●). This 20-pS channel could correspond to a small channel (15 pS in 50 mM KCl symmetrical solution), already mentioned but never fully studied, in sugar beet vacuoles (4).

A strong effect of hydrostatic pressure was found in the whole vacuole experiments. At +50 mV, a small excess in pressure in the pipette increased the current from a few tenths of pA to more than 1,000 pA for some vacuoles (Fig. 3). The opening probability of the 20-pS channel was the only property of this channel affected by pressure (Figs. 2 *a* and 4 *b*). The 70-pS channel properties were not modified by pressure. For the larger pressure used in the experiments, the mean patch current for the 20-pS channel could reach 12 pA (Fig. 2 *b*). With a corresponding value of 0.6 pA for the current in the open state (Fig. 1 *c*), this implies a minimum number of 20 channels in the patch. This large number of channels per active patch seems in contradiction with the fact that  $\sim 1/3$  of the patches were silent in our experiments. It suggests some kind of clustering for these channels. However, we cannot rule out the possibility of an artefact due to the patch pipette (17).

As the channel was being activated by both the suction and excess pressure in the pipette, we tried the effect of  $\text{Gd}^{3+}$ , an inhibitor of stretch activated channels (18–20).  $\text{Gd}^{3+}$  ions were efficient on the cytoplasmic side of the channel in both isolated-patch and whole-vacuole experiments. They strongly reduced the probability of channel opening while they induced a weaker decrease in the channel conductance (Fig. 4). The same kind of block by micromolar  $\text{Gd}^{3+}$  concentration was found on *Xenopus* oocytes, but a larger decrease in conductance has been reported by Franco and Lansman in work on muscle cells (20).

Preliminary measurements do not indicate a strong selectivity cation/anion for this channel whereas previously reported stretch-activated channels are either cation or anion selective (21). This channel does not show the adaptationlike behavior sometimes found with stretch-activated channels (22).

Following different authors (21–24), we used a simple two-state model to fit the data in Fig. 2 *b* and 3 *a*. In this model, the vacuolar current is given by a Boltzmann

distribution:

$$I = \frac{I_{\text{Max}}}{1 + e^{\Delta G_0/KT}} \quad (1)$$

In the equation,  $\Delta G_0$  is the free energy difference between the open and closed states;  $K$  the Boltzmann's constant,  $T$  the absolute temperature, and  $I_{\text{Max}}$ , the maximum value of the vacuolar current.

Sachs and Lecar (25) recently proposed to calculate the free energy in Eq. 1 by considering the open and closed states of the channel as two independent harmonic oscillators. The model predicts both linear and quadratic dependence of the free energy with the applied force, but the relative contribution of the two terms must be evaluated experimentally. In previous experiments, linear or quadratic dependency of free energy with  $P$ , the applied pressure to the patch, were already detected. Our results are consistent with the assumption of a linear dependency of the free energy with  $P$ . It is expressed by the parameter  $\theta$  in the equations given in Fig. legend 2. The parameter  $\theta$  is a measurement of the channel sensitivity to pipette pressure; it is linearly dependent on the patch or vacuolar diameter (26). Values for  $\theta$  obtained from isolated patches range from  $0.33 \text{ kN}^{-1}\text{m}^2$  to  $1.46 \text{ kN}^{-1}\text{m}^2$  (A value for  $\theta$  close to  $1.4 \text{ kN}^{-1}\text{m}^2$  was already measured on *Escherichia coli* [24].) The 4–5-fold change in the  $\theta$  values for isolated patches could be explained by variations in patch diameter (27, 28) but it is difficult to accurately measure it in our experiments. Values for  $\theta$  obtained from whole-vacuole measurements range from  $3.6 \text{ kN}^{-1}\text{m}^2$  to  $25 \text{ kN}^{-1}\text{m}^2$ . This 6–7-fold change in the  $\theta$  value cannot be explained by the variations in vacuolar diameter. The experiments were all performed on vacuoles similar in size (diameter:  $45 \pm 5 \mu\text{m}$ ). A more likely explanation relies on the variations in the mechanical structure of the tonoplast, observed in our preparations (see Preparation of vacuoles) but it was not possible to control this parameter in our experiments. In red blood cells (29), a large scale structure is disrupted by temperature: heating the cells to  $50^\circ\text{C}$  induces a 3–4 $\times$  decrease in the membrane stiffness. There is no correlation between this structure and the gating of channels, but such a correlation was established between the cytoskeleton and a stretch activated channel in chick skeletal muscle (26). We do not know if a matrix in the vacuolar membrane is also used to focus the elastic energy on the channel gate, but if such a matrix exists, it is insensitive to temperature.

Without application of hydrostatic pressure when the vacuolar current was reduced to a small value with  $\text{Ca}^{2+}$  and  $\text{Zn}^{2+}$  ions (Fig. 3 *b*), an osmotic stress resulted in a strong increase in current (Fig. 6 *a*). This increase in

current exhibits several important properties: (a) it occurs with hyperosmotic or hypoosmotic vacuolar solutions (Fig. 6 a); (b) if the 20-pS channel is not already present in a patch without osmotic stress, the patch remains silent after an osmolality change; (c) when already present in a patch, the 20-pS level disappears after an osmolality change in the external medium and a 40-pS level appears at the same time (Fig. 5, a and b); (d) the  $\text{Ca}^{2+}$  sensitive channel is unaffected by osmolality changes; (e) the voltage dependence of the 20- and 40-pS levels are similar (Figs. 1 b, 5 c) they are not closed by depolarization or hyperpolarization of the membrane; and (f) the 20 and 40-pS levels are sensitive to  $\text{Gd}^{3+}$  ions.

These experiments strongly suggest that the 40-pS channel appearing under osmotic stress conditions is the modified 20-pS pressure sensitive channel. To understand the possible mechanism of gating for this channel by an osmotic pressure gradient, we examined two hypotheses.

(a) *The channel is not sensitive to the osmotic pressure itself.* It is the build up of pressure by the water flux resulting from the osmotic gradient which opens pressure activated channels (30). This could be the case in our experiments if the hydrostatic resistance of the patch pipette and membrane were comparable in size. Even in the lack of externally applied pressure, a water flux through the pipette shank could increase the hydrostatic pressure in the patch or in the vacuolar membranes. We discarded this possibility because the largest current induced by an osmotic gradient occurs when there is a water efflux from the vacuole (Fig. 6 a). In this situation, the vacuolar pressure can only decrease in the vacuole, without possibly opening the pressure-activated channels.

(b) *There is a true opening of the channels by the osmotic pressure.* In a model already discussed (8 and 9), the channel is gated by an osmotic gradient between its internal volume and the media facing it. In this model the gradient is generated by the exclusion of some species like sorbitol, from the inner space of the channel, but one may also suspect that a membrane stress could arise if some species were excluded from a region adjacent to the membrane surface (31 and 32). In our experiments, a 0.4 mol/kg isoosmotic change in sorbitol osmolality did not produce a significant increase in the opening probability of the channel, but a 0.2 mol/kg sorbitol osmolality difference between the extracellular and the vacuolar side of the cytoplasm resulted in a > 30-fold increase in the mean patch current (Fig. 1, b and c and 5, c and d). Unfortunately, it seems difficult to predict the effect of an osmotic gradient in these models because in case of a gradient, the osmotic pressure

applied to the channel is not thermodynamically well defined (9).

Our experiments (Fig. 6, a and b) in the gating of an hydrostatic and osmotic pressure-dependent (HOP) channel underline the effect of an osmotic gradient applied to the vacuolar membrane. The magnitude of a vacuolar current depends on the direction of the water flux (Fig. 6 a) induced by this gradient, and a water flux alone can create a vacuolar current (Fig. 6 b). The sign of the current in Fig. 6 b, indicates that the water flux drags more cations than anions, which is in agreement with the selectivity measurements already discussed.

The results reported in this paper strongly suggest a coupling between the HOP channel current and the water flux between the cytoplasmic and vacuolar compartments, but other experiments are needed to quantify this interaction. The coupling between ions and water molecules in a channel has already been used mainly to study the structure of ionic pore in single-file models (33 and 34). Such a coupling in the HOP channel could be important under in vivo conditions. The HOP channel represents a true osmoreceptor which can be activated by a change in the osmotic environment, without the need of a modification in the turgor pressure in the cell.

Received for publication 10 April 1991 and in final form 9 July 1991.

## REFERENCES

- Alexandre, J., J. P. Lassalles, and R. T. Kado. 1990. Opening of  $\text{Ca}^{2+}$  channels in isolated red beet root vacuole membrane by inositol 1,4,5-trisphosphate. *Nature (Lond.)* 343:567-570.
- Berridge, H. J., and R. F. Irvine. 1989. Inositol phosphates and cell signaling. *Nature (Lond.)* 341:197-205.
- Hedrich, R., and E. Neher. 1987. Cytoplasmic calcium regulates voltage-dependent ion channels in plant vacuoles. *Nature (Lond.)* 329:833-836.
- Coyaud, L., A. Kurkdjian, R. T. Kado, and R. Hedrich. 1987. Ion channels and ATP-driven pumps involved in ion transport across the tonoplast of sugar beet vacuoles. *Biochim. Biophys. Acta* 902:263-268.
- Colombo, R., R. Cerana, P. Lado, and A. Peres. 1988. Voltage-dependent channels permeable to  $\text{K}^+$  and  $\text{Na}^+$  in the membrane of *Acer pseudoplatanus* vacuoles. *J. Membr. Biol.* 103:227-236.
- Maathuis, F. J. M., and H. B. A. Prins. 1990. Patch clamp studies on root cell vacuoles of a salt-tolerant and salt-sensitive *Plantago* species. *Plant Physiol.* 92:23-28.
- Falke, L., K. L. Edwards, B. G. Pickard, and S. Misler. 1988. A stretch-activated anion channel in tobacco protoplasts. *FEBS (Fed. Eur. Biochem. Soc.) Lett.* 237:141-144.
- Finkelstein, A. 1987. Water movement through lipid bilayers, pores, and plasma membranes, theory and reality. In *Distinguished lectures series of the Society of General Physiologists*, Vol. 4. John Wiley and Sons, New York.

9. Zimmerberg, J., F. Bezanilla, and V. A. Parsegian. 1990. Solute inaccessible aqueous volume changes during opening of the potassium channel of the squid giant axon. *Biophys. J.* 57:1049–1064.
10. Hamil, O. P., A. Marty, E. Neher, B. Sakmann, and F. J. Sigworth. 1981. Improved patch-clamp techniques for high-resolution current recordings from cells and cell-free membrane patches. *Pfluegers Arch. Eur. J. Physiol.* 391:85–100.
11. Mittman, S., D. G. Flaming, D. R. Copenhagen, and J. H. Belgium. 1987. Bubble pressure measurement of micropipet tip outer diameter. *J. Neurosci. Methods.* 22:161–166.
12. Martinac, B., M. Buechner, A. H. Delcour, J. Adler, and C. Kung. 1987. Pressure-sensitive ion channel in *Escherichia coli*. *Proc. Natl. Acad. Sci. USA.* 84:2297–2301.
13. Leigh, R. A., and D. Branton. 1976. Isolation of vacuoles from root storage tissue of *Beta vulgaris L.* *Plant Physiol.* 58:656–662.
14. Ringbom, A. 1967. In *Les complexes en Chimie Analytique*. Dunod, editor. Dunod, Paris. 38–40.
15. Hedrich, R., and A. Kurkdjian. 1988. Characterization of an anion-permeable channel from sugar beet vacuoles: effect of inhibitors. *EMBO (Eur. Mol. Biol. Organ.) J.* 7:3661–3666.
16. Sakmann, B., and E. Neher. 1983. Geometric parameters of pipettes and membrane patches. In *Single channel recording*. B. Sakmann and E. Neher, editors. Plenum Publishing Corp., New York. 37–51.
17. Milton, R. L., and J. H. Caldwell. 1990. How do patch clamp seals form a lipid bleb model. *Pfluegers Arch. Eur. J. of Physiol.* 416:758–765.
18. Yang, X., and F. Sachs. 1989. Block of stretch-activated ion channels in *Xenopus* oocytes by gadolinium and calcium ions. *Science (Wash. DC).* 243:1068–1070.
19. Filipovic, D., H. Sackin. 1991. A calcium-permeable stretch-activated cation channel in renal proximal tubule. *Am. J. Physiol.* 260:119–129.
20. Franco, A., and J. B. Lansman. 1990. Stretch-sensitive channels in developing muscle cells from a mouse cell line. *J. Physiol. (Lond.)* 427:361–380.
21. Sachs, F. 1988. Mechanical transduction in biological systems. *CRC Crit. Rev. Biomed. Eng.* 16:141–169.
22. Gustin, M. C., X. L. Zhou, B. Martinac, and C. Kung. 1988. A mechanosensitive ion channel in the yeast plasma membrane. *Science (Wash. DC).* 242:762–765.
23. Howard, J., W. M. Roberts, and A. J. Hudspeth. 1988. Mechano-electrical transduction by hair cells. *Annu. Rev. Biophys.* 17:99–124.
24. Martinac, B., J. Adler, and C. Kung. 1990. Mechanosensitive ion channels of *E. coli* activated by amphipaths. *Nature (Lond.)*. 348:261–263.
25. Sachs, F., and H. Lecar. 1991. Stochastic models for mechanical transduction. *Biophys. J.* 59:1143–1145.
26. Guharay, F., and F. Sachs. 1984. Stretch-activated single ion channel currents in tissue-cultured embryonic chick skeletal muscle. *J. Physiol. (Lond.)*. 352:685–701.
27. Sokabe, M., and F. Sachs. 1990. The structure and dynamics of patch-clamped membranes: a study using differential interference contrast light microscopy. *J. Cell Biol.* 111:599–606.
28. Sokabe, M., F. Sachs, and Z. Q. Jing. 1991. Quantitative video microscopy of patch clamped membranes stress, strain, capacitance, and stretch channel activation. *Biophys. J.* 59:722–728.
29. Evans, E. A., R. Waugh, and L. Melnick. 1976. Elastic area compressibility modulus of red cell membrane. *Biophys. J.* 16:585–595.
30. Edwards, K. L., and B. G. Pickard. 1987. Detection and transduction of physical stimuli in plants. In *The Cell Surface in Signal Transduction*. NATO ASI series Vol. H12. E. Wagner, H. Greppin, and B. Miller, editors. Springer-Verlag, Berlin. 41–66.
31. Yamazaki, M., S. Ohnishi, and T. Ito. 1989. Osmoelastic coupling in biological structure: decrease in membrane fluidity and osmophobic association of phospholipid vesicles in response to osmotic stress. *Biochemistry.* 28:3710–3715.
32. Ito, T., M. Yamazaki, and S. Ohnishi. 1989. Osmoelastic coupling in biological structures: a comprehensive thermodynamic analysis of the osmotic response of phospholipid vesicles and a reevaluation of the “dehydration force” theory. *Biochemistry.* 28:5626–5630.
33. Rosenberg, P. A., and A. Finkelstein. 1978. Water permeability of gramicidin A-treated lipid bilayer membranes. *J. Gen. Physiol.* 72:341–350.
34. Rosenberg, P. A., and A. Finkelstein. 1978. Interaction of ions and water in gramicidine A channels. Streaming potentials across lipid bilayer membranes. *J. Gen. Physiol.* 72:327–340.